Dependence of Particle Transport on Heating Profiles in ASDEX Upgrade

J. Stober[1], R. Dux[1], O. Gruber[1], L. Horton[1], P. Lang[1], R. Lorenzini[2], C. Maggi[1], F. Meo[1], R. Neu[1], J.-M. Noterdaeme[1], A. Peeters[1], G. Pereverzev[1], F. Ryter[1], A.C.C. Sips[1], A. Stäbler[1], H. Zohm[1], and the ASDEX Upgrade Team

[1] *MPI für Plasmaphysik, EURATOM Association, D-85748 Garching, GERMANY*
[2] *Consorzio RFX, Associazione EURATOM-ENEA sulla Fusione, I-35127 Padova, ITALY*
e-mail: Stober@ipp.mpg.de

Abstract: The behaviour of the density profiles in ASDEX Upgrade can be well described with the assumption of $D \propto \chi$ and a pinch of the order of the neoclassical Ware-pinch. The latter is estimated from slowly equilibrating density profiles. The assumption of $D \propto \chi$ has been succesfully tested by varying the heat deposition profile making use of on/off-axis ICRH and ECRH: due to the generally observed self-similarity of the temperature profile such variations of the heat flux profile have a strong effect on the χ-profile and on the D-profile if the above assumption is correct. The corresponding variations of the density profiles have indeed been observed. The model is also capable of describing the decay of the density profile after injecting a train of pellets. The anomalous transport of impurities is also increased with central heating. Central ICR or ECR heating are therefore now routinely used to control the density peaking and its negative effect on the stability of NTMs as well as to control the impurity transport in ASDEX Upgrade.

Density peaking at high densities: Experiments and model

The peaking of density profiles on a time scale much longer than τ_E has been observed recently in various tokamaks for moderately NBI heated plasmas at high density [1,2,3]. These experiments are done by operating a type-I ELMy H-mode close to the high density transition to type-III ELMs. The pedestal parameters are kept constant during the peaking process. In ASDEX Upgrade it has been observed that this slow density peaking does not occur if half of the NBI power is substituted by central ICRH resulting in a flat density profile. This means, that a higher central value of D or a smaller particle pinch are required for the mixed NBI/ICRH case than for the peaked density profile with pure NBI. The heating profile is much more peaked with central ICRH than with NBI heating but the temperature profiles are very similar (in agreement with the generally observed T-profile stiffness in ASDEX Upgrade). Therefore the heat conductivity χ increases significantly in the plasma center when applying central ICRH. This leads to the assumption that D might increase with χ. A model assuming a radially constant ratio of D/χ_{eff}^{exp} and a pinch term in the order of the neoclassical Ware pinch has been set up using the ASTRA code [4]. Comparing pure NBI heating (slow density peaking) to partially (50%) heating with central ICRH (steady state flat density profile) a value of $D/\chi_{eff} \approx 0.12$ and $v \approx 1.5 \times v_{Ware}$ allow a good description for both heating profiles (taking the density at the top of the pedestal as boundary condition). The observed peaking with long time constants corresponds to small central diffusion coefficients and a pinch term in the range of the neoclassical Ware pinch. Significantly higher pinch terms cannot reproduce the long time scale. These results have been published in [2]. More recently, we realized that the neoclassical ion heat-conductivity contributes significantly to χ_{eff} in the case of pure NBI heating, i.e. for the inner half of the plasma $\chi_{eff} = 0.5(\chi_e + \chi_i) \approx \chi_{i,neo}$. Since the assumption $D \propto \chi$ is based on the idea, that the turbulence generating the anomalous heat flow can also affect the particle flow, the non-turbulent heat-flow due to $\chi_{i,neo}$ should be excluded. This leads to the definition of a turbulent effective heat conductivity $\chi_{eff}^{turb} = 0.5(\chi_e + \chi_i - \chi_{i,neo})$ which should better describe the strength of the transport driving turbulence (Note that $\chi_{e,i}$ cannot be estimated separately since the heat exchange cannot be determined with sufficient accuracy). For the strong peaking with NBI $\chi_{eff}^{turb} \approx 0.5\chi_{eff}$, resulting in $D/\chi_{eff}^{turb} \approx 0.25$. A lower limit for D is given by $D_{min} = D_{neo}$. The corresponding transport simulations are shown in [5]. Some doubts on the interpretation of the above reported experiments remained, based on the suspicion that the particle

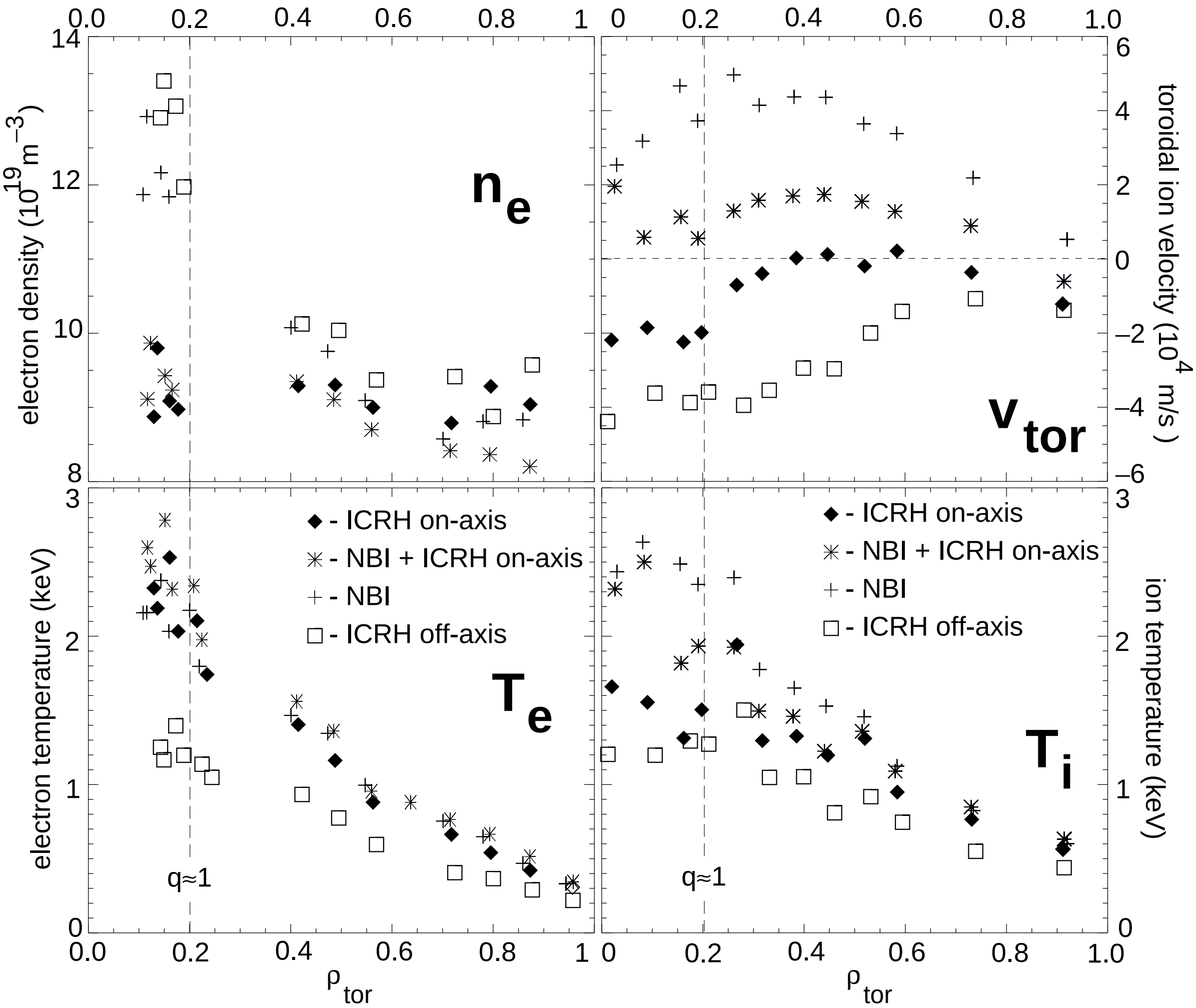

Figure 1: Electron density, temperature and toroidal rotation (v_{tor}) profiles for different heating scenarios: on-axis ICRH (5 MW) #15062, on-axis ICRH (2.5 MW) mixed with NBI (2.5 MW)#15061, NBI(5 MW) #15060, and off-axis ($\rho \geq 0.65$) ICRH (4.2 MW) #15122. $I_p = 1$ MA, $q_{95} \approx 4.3$, $\delta = 0.32$. The v_{tor} values may have a significant constant offset due to uncertainties of the absolut wavelength calibration of several 10^4 m/s. For the density profiles the zero is suppressed.

fueling with NBI could be responsible for the peaking, even if a flat profile had already been observed when reducing the NBI fueling only by 50%. To check this point similar experiments with only ICR heating were planned to exclude any internal particle sources. This requires the operation of the ICRH system at its technical limits and is only possible due to the use of 3 dB couplers to allow operation despite strong reflections due to strong ELMs as reported in [6]. Since the ASDEX Upgrade ICRH system can operate at two frequencies the toroidal field B_t could be kept constant within 5% when comparing on-axis (30 MHz, 2.1 T) and off-axis (40 MHz, 2.2 T) heating. This is important to exclude the influence of q_{95} which is known to influence the density peaking in the NBI scenario [1]. In Fig. 1 four different heating scenarios are compared. Full on-axis ICRH, full NBI, a one-to-one mixture of NBI and central ICRH (total additional power in these cases: 5 MW) as well as off-axis ICRH (4.2 MW only, due to technical limits). All discharges show type-I ELMs and an H-factor above 1.0 (ITER-H98). The density profiles in the NBI and off-axis ICRH cases are peaked while those with central ICRH are flat. The temperature profile shape is almost unchanged, especially for the electron temperature whereas the ion temperature is somewhat flatter in the center for the ICR heating, especially for the on-axis case. This is in contrast to the rigid stiffness observed so far for the ion temperatures in NBI heated plasmas in ASDEX Upgrade [7].It is also striking that in the case of off-axis ICR heating the T-profiles remain close to the self similar shape. Transport analysis reveals that in this case $\chi_{i,neo}$ can account for the full heat transport in the inner half of the plasma. This would require that $T_e - T_i \approx 200$ eV in the plasma center to transfer the electron heating locally into the ion channel which is possible within the error of the data. The power deposition of the ICRH which enters crucially in such an analysis was calculated with the TORIC code [8]. The direct electron heating by ICR in the plasma center is of the same size as the ohmic heating. The central value of $\chi_{i,neo} \approx 1.5\mathrm{m}^2/\mathrm{s}$ is based on guiding center particle orbit calculations [9]. Since any remaining turbulent energy transport is hidden in the experimental uncertainties, $D_{min} = D_{neo} = \sqrt{m_e/m_i}\chi_{i,neo} \approx 0.025\mathrm{m}^2/\mathrm{s}$ determines the particle transport in this low turbulence region. Fig. 2 shows the evolution of the density profile which is well described by our model using $D/\chi_{eff}^{turb} = 0.25$ in the outer half of the plasma and the Ware pinch.

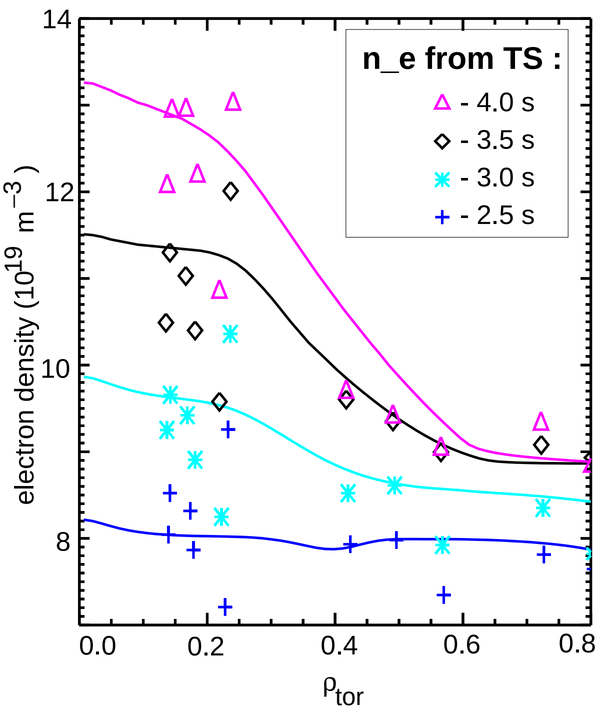

Figure 2: Electron density for the off-axis ICRH scenario (see fig. 1). Symbols represent Thomson scattering measurements, lines correspond to modelling results for the same time points. The boundary conditions for the model are nominally at the separatrix, but are adjusted such that the density values at $\rho_{tor} = 0.8$ are matched. D and v_{in} can be separated due to the time evolution within a factor ≈ 2.

A similar experiment with on-axis and off-axis ICR heating has been performed on Alcator C-mod where also a slow density peaking in the off-axis case has been observed [10]. The authors assume that the effect is related to the observed changes in the plasma rotation. Therefore we show in fig. 1 also the plasma rotation. In the pure ICRH cases the first frame of the CX recombination spectroscopy after switching back to NBI is shown. There is indeed a clear difference between on- and off-axis ICRH but the difference between the NBI and the off-axis ICR heating is twice as large. This either indicates that the rotation plays a minor role for the density peaking in ASDEX Upgrade or that the nature of the peaking process is different in both cases.

Application to pellet fuelled H-modes

The assumptions on particle transport have been tested to describe the evolution of the density profile after a train of pellets. This study dealt with a hydrogen plasma at lower triangularity $\delta \approx 0.15$ and lower plasma current $I_p = 0.8$ MA [5]. Therefore the energy confinement was significantly worse and $\chi_{eff}^{turb} \approx \chi_{eff} \gg \chi_{i,neo}$. As described in [5,11] the density profile before the pellet injection can be reproduced using $0.2 < D/\chi_{eff} < 0.25$ and the Ware pinch. The density decay and the flattening of the density profile after injecting a train of fast pellets from the high field side is also found to be compatible with an unchanged ratio of D/χ_{eff}^{turb} and with the Ware pinch in the confinement region. Here we did not try to model the first 5 ms after the last pellet which are known to be dominated by convection due to strong ELMs [12]. We also had some difficulties to include the effect of one big single sawtooth on the density profile which regularly occurs under these conditions and did not fit well into our sawtooth model.

Test with ECR heated L-modes

Further insight into the underlying physics is expected from low density experiments allowing to separate ion and electron channel: First results show that the model is also applicable to explain the density profile flattening with ECRH as compared to the ohmic case [13]. A detailed analysis of these data shows that mainly χ_e is affected by the change of the electron heat flux. The ohmic case requires $D/\chi_e \approx 0.15$ and the case with central electron heating $D/\chi_e \approx 0.20$ using only the Ware pinch in both cases. Experiments comparing on- and off-axis ECRH for heat-transport studies [14] have been used to test the particle transport model but the results are not conclusive: the observed change of the density profile is small but in the expected direction. Assuming $D/\chi_e \approx 0.20$ the expected increase of the central density by shifting the ECRH deposition from $\rho_{tor} = 0.35$ to $\rho_{tor} = 0.65$ would be from 2.0×10^{19} m^{-3} to approximately 2.5×10^{19} m^{-3}, which is within the uncertainty of the data. The small effect is due to the low value of the Ware pinch at high electron temperature and low density, since it is driven by the loop voltage.

Relations to impurity transport

The influence of the heat-flux profile on the impurity transport has also been studied: In those discharges described in fig. 1 which are heated by ICR only, silicon has been injected into the plasma by laser-blow-off of thin-film Si samples. The anomalous diffusivity of Si in the plasma center is found to be significantly larger for the case with central ICRH as compared to off-axis ICRH, whereas the pinch velocities in the confinement region are close to the neoclassical values [15]. This fits well to the behaviour of the concentration of heavy impurities (mainly tungsten due to the W coated central column of ASDEX Upgrade [16]): accumulation provoked with off-axis heating can be significantly reduced and kept at a low level by application of additional central ECRH [17,18,19].

Impact on plasma operation

The peaking of the density profile can disturb plasma operation in several ways. The neoclassical impurity pinch increases with the peaking of the density profile and also neoclassical tearing modes (NTMs) are less stable in plasmas with the same β but stronger density peaking [13]. The slow peaking process may not reach equilibrium but may lead to the loss of sawteeth followed by accumulation of impurities and a radiative collapse [1,2,3]. To avoid these unfavourable effects central ICRH is essential for some important scenarios in ASDEX Upgrade: H-modes with $q_{95} = 3$ at increased δ show an uncontrollable density peaking with NBI only, perhaps due to the high natural density which we generally observe when operating at $\delta \geq 0.3$. Steady state operation could only be reached with partial central ICR heating at the corresponding $B_t \approx 2$ T. During reversed I_p operation with NB counter injection, the NBI heating profile is even more off-axis due to outward going orbits of the trapped fast ions. The density peaking is more pronounced so that any steady state operation at $\delta \geq 0.3$ requires central ICRH. Also, so called "improved H-modes" in ASDEX Upgrade can be run at $\delta \geq 0.3$ only with on-axis ICRH. These discharges are low density H-modes with fishbones as central MHD and no sawteeth. This leads to an additional peaking of the central density profile, which triggers an NTM (even without a sawtooth induced seed-island) if it is not reduced with central ICRH [20,21].

Conclusion

The old idea of a close relation between D and χ has been used successfully to describe the behaviour of the density profiles. It relates the shape of the density profile closely to the heat flux profile since the shape of the temperature profiles remains almost unchanged due to the dependence of the underlying transport on a critical value of $\nabla T/T$ [7,14]. The same mechanism affects also the impurity transport. We generally find $0.15 \leq D/\chi_{eff}^{turb} \leq 0.25$ when using only the Ware pinch. The uncertainty of this ratio is about 0.05 for a single simulation. From theoretical considerations this ratio is not expected to be universal in all cases, and it can be regarded as challenge for a theory to reproduce this tendency of our simple model. An issue of controversial discussion is the existence of additional turbulence driven pinch terms [22]. We can only determine the pinch for the high density cases which show a slow time evolution. For these, additional pinch terms can only be in the order of the Ware pinch. In all other cases we analysed only the steady state situation and we could have used higher pinches, requiring higher values of D/χ. Independent of this question, it is clearly demonstrated that central heating, which will be also dominant in a fusion reactor, facilitates plasma operation in terms of density profile control, impurity control and stability against NTMs.

References

[1] MAHDAVI, M. A. et al., Nucl. Fusion **42** (2002) 52.
[2] STOBER, J. et al., Nucl. Fusion **41** (2001) 1535.
[3] VALOVIC, M. et al., Plasma Phys. Controlled Fusion **44** (2002) 1911.
[4] PEREVERZEV, G. and YUSHMANOV, P. N., ASTRA Automated System for TRansport Analysis in a tokamak, Technical Report 5/98, IPP, Garching, Germany, 2002.
[5] LORENZINI, R. et al., *Europhysics Conference Abstracts (CD-ROM, Proc. of the 29th EPS Conference on Controlled Fusion and Plasma Physics, Montreux 2002)*, volume 26B, pages P–1.041, Geneva, 2002, EPS.
[6] NOTERDAEME, J.-M. et al., *Fusion Energy 1998*, volume 2, pages 659–662, Vienna, 1999, IAEA.
[7] TARDINI, G. et al., Nucl. Fusion **42** (2002) 258.
[8] BRAMBILLA, M., Plasma Phys. Controlled Fusion **41** (1999) 1.
[9] BERGMANN, A. et al., Phys. Plasmas **8** (2001) 5192.
[10] RICE, J. E. et al., Nucl. Fusion **41** (2001) 277.
[11] STOBER, J. et al., Nucl. Fusion , to be submitted at this conference.
[12] LANG, P. T. et al., Nucl. Fusion **41** (2001) 1107.
[13] STOBER, J. et al., Plasma Phys. Controlled Fusion **43** (2001) A39.
[14] RYTER, F. et al., Nucl. Fusion , to be submitted at this conference.
[15] DUX, R. et al., Nucl. Fusion , to be submitted.
[16] ROHDE, V. et al., Nucl. Fusion , to be submitted at this conference.
[17] NEU, R. et al., Plasma Phys. Controlled Fusion **44** (2002) 1021.
[18] STOBER, J. et al., Plasma Phys. Controlled Fusion **44** (2002) A159.
[19] DUX, R. et al., J. Nucl. Mater. , submitted, issue of PSI 2002.
[20] STÄBLER, A. et al., *Europhysics Conference Abstracts (CD-ROM, Proc. of the 29th EPS Conference on Controlled Fusion and Plasma Physics, Montreux 2002)*, volume 26B, pages O–5.03, Geneva, 2002, EPS.
[21] SIPS, A. C. C. et al., Plasma Phys. Controlled Fusion submitted, invited paper EPS 2002.
[22] WEILAND, J., *Europhysics Conference Abstracts (CD-ROM, Proc. of the 28th EPS Conference on Controlled Fusion and Plasma Physics, Madeira 2001)*, volume 25A, pages 633–636, Geneva, 2001, EPS.